EXPERIMENTAL STUDY OF THE CONDUCTED ACTION POTENTIAL IN CARDIAC PURKINJE STRANDS

MARC K. WALTON AND HARRY A. FOZZARD
Departments of The Pharmacological and Physiological Sciences and of Medicine, The University of Chicago, Chicago, Illinois 60637

ABSTRACT Conduction velocity is a complex physiological process that integrates the active and passive properties of the excitable cell. The relations between these properties in determining the conduction velocity are not intuitively obvious, and models have been used frequently to illustrate important relationships. To study the relationships of important parameters and to evaluate commonly used models, we changed conduction velocity experimentally in sheep cardiac Purkinje strands by reducing extracellular Na systematically. Cable analyses were also performed to obtain passive membrane and cable properties. Resting membrane resistance and capacitance did not change, nor did core resistance. Active properties measured in addition to conduction velocity included maximal upstroke velocity, action potential height, time constant of the foot, peak inward current, and upstroke power. With reduction in extracellular Na, all of these parameters of the action potential changed nonlinearly and not in direct proportion to the change in conduction velocity. The only simple relation found was a linear relationship between maximal upstroke velocity and peak inward current, normalized by the capacity of the foot. Models based on the cable equation and the wave equation offer a basis for quantitative analysis of conduction, and these data can be used to test the models.

INTRODUCTION

Communication in nerve and striated muscle relies on the propagated action potential. It is a complex process that involves all of a tissue's active and passive properties. Although the ionic basis of the membrane action potential in some nerves is well known (Hodgkin and Huxley, 1952), the relationship of the basic properties to the characteristics of the conducted action potential is not well understood.

The activated, transmembrane ionic current (I_i) is the driving influence for conduction, and it interacts with the passive membrane and cable properties of the tissue to yield a steady, balanced, state of conduction (Fozzard, 1979). The characteristics of the ionic currents are best studied under nonphysiologic conditions, such as a voltage clamp, which are difficult to relate to the conducted situation. As a result, experimental studies of conduction have usually focused on readily observable properties of conduction, such as velocity (θ), maximal upstroke velocity ($\dot{V}_{max}$), action potential height (V_{pk}), and others. The relationships between the ionic current and these easily measured properties are not intuitively obvious. A combination of experimental study and mathematical modeling will be required to clarify them on a quantitative basis.

This is an experimental study of parameters of conduction during systematically induced changes in propagation. Few prior studies of conduction have provided information on ionic current. This study does so by a method similar to the phase-plane method used by Jenerick (1963, 1964*a*, *b*). Cardiac Purkinje strands were used in the study because they have several characteristics that make them particularly interesting and useful. In the heart they are specialized for fast conduction with a wide margin of safety, and will conduct over a wide range of conditions. Although their passive properties are complex (Fozzard, 1966; Freygang and Trautwein, 1970), they have been well studied. This aids in reliably utilizing the methods described here. While these results were obtained in heart cells, most of the properties and results can be generalized to other conducting tissues (Fozzard, 1979).

In this study, propagation is altered in a systematic manner by changing the sodium concentration of the external solution. The basic passive cable properties did not change with reduced external sodium. Ionic current correlated well with $\dot{V}_{max}$. However, θ was not related to either $\dot{V}_{max}$ or ionic current by a simple proportionality, indicating that other factors are involved in the relationship. These data are used in a companion study to aid in the evaluation of models of conduction.

GLOSSARY

a	Radius of the cylindrically modeled fiber
a_i, a_o	Intracellular and extracellular activities of an ion species, specifically implied Na activity
C_m	Low frequency capacitance per unit cylindrical surface area
C_f	Capacitance filled during foot of upstroke; capacitance per unit cylindrical surface area
G	Membrane conductance per unit cylindrical surface area
$\hat{I}$	Peak inward ionic current (I_i) during upstroke

I_i	Ionic current density across membrane ($\mu A/cm^2$ cylindrical surface area); also refers to ionic current density during entire upstroke
K	Rate constant of rise of action potential, = $1/\tau_f$ $(1/t)$
P	Power of ionic current during entire upstroke = $\int I_i dV \Big|_{V_o}^{V_{pk}}$
R_i	Specific resistivity of intracellular fluid (Ω – cm)
R_m	Specific membrane resistance (Ω – cm^2 cylindrical surface area)
t	Time
V	Membrane potential (inside-outside); usually a relative potential where values are shifted so that resting potential is 0 mV.
$\overline{V}$	Potential at which $\dot{V}_{max}$ occurs
V_{pk}	Peak membrane potential, occurs at end of upstroke
V_r	Resting membrane potential
$\dot{V}$	dV/dt, especially as entire curve during upstroke
$\dot{V}_{max}$	Maximum upstroke velocity; peak value of $\dot{V}$ during upstroke
$\ddot{V}$	d^2V/dt^2; second derivative of voltage in time at one, fixed position
θ	Conduction velocity (meters per second)
τ_f	Time constant of rise of foot of action potential, = $1/K$
τ_m	Low frequency membrane time constant.

METHODS

Tissues and Equipment

Hearts were obtained from freshly slaughtered sheep and transported to the laboratory in cooled Tyrode's solution. Long free-running Purkinje strands were dissected and placed in Tyrode's solution containing (in millmoles per liter) NaCl 137, KCl 5.4, $CaCl_2$ 1.8, $MgCl_2$ 1.05, $NaHCO_3$ 22, NaH_2PO_4 2.4, glucose 11. The solution was gassed with a 95% O_2, 5% CO_2 mixture, and had a pH of 7.2–7.4. The strands were placed in a lucite chamber and held in position by 6-0 nylon suture lightly touching on top. Temperature was monitored with a thermistor probe (Yellow Springs Instrument Co., Yellow Springs, OH) and maintained at 36°–37°C, ± 0.5°C.

Glass microelectrodes were filled with 3 M KCl, except those for intracellular current passage, which were usually filled with 2 M potassium citrate. Electrodes utilized had resistances of 10–20 MΩ. Membrane potential signals from the microelectrodes were led to high-input impedance voltage followers (picometric model 181, Instrumentation Laboratory, Inc., Lexington, MA). These voltage followers also have a capacity neutralization capability that was adjusted to give a fast response to a square step without ringing.

The bathing solution was virtually grounded using an operational amplifier (National Instrument Co., Baltimore, MD, model LH0042) in a current-to-voltage converter mode and connected to the tissue bath by an Ag/AgCl electrode in polyethylene tubing filled with an agar–3 M KCl gel (3% wt/vol). The circuit also functioned to produce a voltage output proportional to the current passed through the tissue bath. All signals were displayed on a dual beam oscilloscope (model D-44, Tektronix, Inc., Beaverton, OR) and recorded on 35 mm film using a Kymograph camera (model C4, Grass Instrument Co., Quincy, MA).

Mathematical Basis for Ionic Current Calculation

Most of the experimental measures of a Purkinje strand can be obtained by well-known methods. However, obtaining the ionic current trajectory during the upstroke of the action potential is not commonly done. The method we used is similar to that of Jenerick (1963, 1964*a*, *b*), although the specific details of its application are different.

The first step is to treat the Purkinje fiber using standard cable theory (Hodgkin and Rushton, 1946), with the assumption of a uniformly conducting action potential producing

$$\frac{a}{2R_i\theta^2} \cdot \frac{\partial^2 V}{\partial t^2} = C_m \frac{\partial V}{\partial t} + I_i \tag{1}$$

where a is the cable's radius, R_i the axial resistivity, and C_m the capacitance per unit surface area. This equation has been utilized often in other ways. For example, if one considers the foot of the action potential, where the sodium conductance has not yet increased and membrane resistance remains high, then V/R_m may be substituted for I_i, and the equation solved for V as the unknown (Cole and Curtis, 1938; Rosenblueth et al., 1948), to arrive at the Tasaki and Hagawara (1957) relation for K, the rate constant of the action potential foot:

$$K = 2R_i\theta^2 C_m/a. \tag{2}$$

If, however, this equation is utilized with the $V(t)$ curve as a known entity, then the ionic current curve may be obtained by the application of the first two time derivatives of the $V(t)$ curve:

$$I_i = \frac{a}{2R_i\theta^2} \frac{d^2V}{dt^2} - C_m \frac{dV}{dt}. \tag{3}$$

The other parameters, R_i, θ, C_m, and a are easily obtained.

In this formulation, C_m is the capacitance of the membrane that is charged during the upstroke of the action potential. In cardiac Purkinje fibers, this capacitance is frequency dependent (Fozzard, 1966; Levin and Fozzard, 1981). The Tasaki-Hagiwara relation can be used to calculate this capacitance, called C_f to distinguish it from the C_m value obtained in low frequency analysis.

Experimental Procedure

Strands were impaled with three microelectrodes: a current-passing electrode near a loop of thin suture tied around the strand at one end (to produce a known and identified site of injury), a voltage-recording electrode ~500 μm from the first, and a second voltage electrode ~1 mm further along the strand. To determine the steady-state cable parameters, a constant-current pulse of 200 ms duration and of intensity to produce ~5 mV deflection at the first voltage electrode was passed through the current electrode. The virtual ground (signal proportional to current) and two voltage electrode signals were recorded. The strand was then stimulated by bipolar electrodes at the end opposite the electrodes with a stimulus of ~200 μs duration and intensity slightly suprathreshold from a stimulus isolator (model MkIV, Devices Sales Ltd., Welwyn Garden City, Hertfordshire, England) at a rate of 0.4 Hz. One of the voltage traces was displayed on the oscilloscope to monitor a complete action potential. The voltage signal was then led into an amplifying-filtering-differentiating unit. This unit produced signals proportional to the voltage, and to the first and second time derivatives during the action potential upstroke. The filter stage consisted of three separate modules, one of which could be selected into the circuit. Each module had the frequency response characteristics of an eight-pole Butterworth filter (Burr-Brown, Tucson, AZ), with corner frequencies of 18, 11, and 6 kHz. These were chosen to give flat amplitude response (>99%) and linear phase shift (constant time delay with frequency change, ±2.5 μs) from low frequencies to 16.3, 7.4, and 3.1 kHz. These limits were chosen on the basis of approximate frequency requirements of upstrokes of 1,000 V/s, 120 mV height; 500 V/s, 120 mV; 200 V/s, 100 mV. In practice, the second derivative trace was displayed and the lowest filter that produced no distortion was used.

The outputs from the filter and both differentiators were displayed and recorded. The input of the second differentiator was then switched to the other voltage electrode and the two first derivative signals displayed and recorded to obtain conduction velocity. The entire system was checked for frequency response and calibrated both as each individual section and by passing signals into the tissue bath so that it had to pass through the

microelectrode and all amplifying components before being displayed. After all required signals were recorded, the Tyrode's solution was changed, the stimulated strand allowed to equilibrate for ~10 min, and the sequence of data recording repeated.

The modified Tyrode's solutions were made by substituting tetramethylammonium chloride (TMA) (Aldrich Chemical Co., Inc., Milwaukee, WI) for NaCl in equimolar amounts to produce solutions containing 50, 35, 25, or 20% of the normal Tyrode's 161 mM Na. Modified solutions were used successively with occasional returns to 161 mM Na solution. By using several steps of lowered sodium, several progressively slower states of conduction should be obtained for analyses. TMA was chosen as the sodium replacement because of advantages over some of the other substances commonly used to maintain osmolarity. TMA has been shown to be unable to pass through the sodium channel of several tissues (Cahalan and Begenisich, 1976; Hille, 1971; Campbell, 1976). Although it has recently been shown to be a blocker of sodium channels when on the cytoplasmic side (Horn et al., 1981), TMA does not have this effect externally (Hille, 1975). By being impermeant and inert it substitutes for sodium without loss of conductivity in the bathing solution or other unwanted effects.

Data Analysis

Standard steady state three-microelectrode cable analysis was utilized to calculate values for R_i, R_m, C_m, and τ_m according to the relations from linear cable theory (Hodgkin and Rushton, 1946; Weidmann, 1952; Fozzard, 1966).

Maximal velocity of the upstroke, $\dot{V}_{max}$, was measured as the peak height of the dV/dt trace, and the potential at $\dot{V}_{max}$, $\overline{V}$, as the point on the voltage trace at the moment $\dot{V}_{max}$ occurred. The early portion of the voltage trace was manually measured at equally spaced intervals of time and plotted as $\ln(V)$ vs. time. The best straight line was drawn by eye through them and its slope determined and used as K $(-1/\tau_f)$. Conduction velocity was determined as the distance between the two voltage electrodes divided by the conduction delay of the moments of $\dot{V}_{max}$ at each electrode. The measured delay was adjusted for the additional delay introduced by the filter section that one signal passed through. From the obtained values of R_i, a, θ, and K, C_f was calculated as described previously $(-aK/2R_i\theta^2)$.

The second derivative signal was generally too noisy to be used directly in the manner previously described (Eq. 3). The method chosen to alleviate this problem was to digitize the dV/dt record using an electronic digitizer (model 762, Wang Laboratories, Inc., Lowell, MA) and fit a smooth, continuous curve to the data. The equation for this curve and its derivative were used to provide $\dot{V}$ and $\ddot{V}$ values for calculating I_i. Several methods of curve fitting were tried, and it was found that the best of them was to use a modified logit transform. In this method the data was transformed from $V(t_i)$ to $T(t_i) = \ln\{[D/\dot{V}(t_i) + B] + A\}$. The $T(t_i)$ points were fitted to a polynomial in variable $t[P(t)]$. The length (degree) of the polynomial was determined largely by the σ^2 method (Ralston, 1965). The parameter D was set to ~101% of $\dot{V}_{max}$. A and B were determined by trial and error to give the best fit of the polynomial to the data, with special emphasis upon the region of higher $\dot{V}$. The $\dot{V}$ curve was then obtained from the inverse transform $\dot{V}(t) = D \cdot [e^{P(t)} - A]^{-1} - B$ and $\ddot{V}$ from its derivative. These were then used to give a curve for $I_i(t)$ as described previously (Eq. 3). It should be emphasized that these curves are purely empirical. They have no known theoretical significance as a whole, nor do the various constants within them or the transform have any known meaning outside of their ability to replicate the recorded data.

RESULTS

Cable and Upstroke Parameters

The useful information obtained from a single experiment consisted of the various cable and upstroke characteristics as functions of the external sodium, and families of $V(t)$ and $\dot{V}(t)$ curves. $\ddot{V}(t)$ curves were obtained in most cases, but usually not in the lowest Na_o solutions, because of the poor signal-to-noise ratio. The actual values, either in control solution or in the Na-deficient solutions, were generally not the same in different experiments. To give each experiment equal weighting when looking at the altered behavior, each experiment was normalized by the average value in full sodium solution before averaging all the experiments together. Only one fiber continued to conduct in 20% Na_o. Because this is a single value and not an average of all the experiments, it is not shown on figures of average behavior.

The average unnormalized values in control solution along with the average normalized behavior in low-Na solutions are listed in Tables I and II. Fig. 1 demonstrates that the cable parameters R_i, R_m, and C_m remained relatively unchanged. Although there appeared to be an increase in R_m in 50% Na, it is not statistically significant, due to a large variance. C_f, however, did show a marked and significant rise as Na_o decreased. The ratio of C_f/C_m in control solution was 0.211. This is similar to previously reported values for mean C_f/mean C_m of 0.188 (Fozzard, 1966) and 0.192 (Fozzard and Schoenberg, 1972).

The action potential parameters $\overline{V}$, V_{pk}, θ, K, and $\dot{V}_{max}$ (Fig. 2) all fell uniformly as Na_o was lowered. Each parameter had a different sensitivity to lowered Na_o; $\overline{V}$ had the least and $\dot{V}_{max}$ the most. It should be noted that at the lowest Na_o that sustained conduction, the parameters were still some significant distance from zero.

The $V(t)$ and $\dot{V}(t)$ curve families are most easily represented as phase-plane diagrams (Fig. 3) obtained by plotting the $\dot{V}(t)$ value with the corresponding $V(t)$ value.

TABLE I
EFFECT OF LOWERED $[Na]_o$ ON RESTING PROPERTIES

	Mean value (n = 5)	Percent Na 100 (n = 13)	50 (n = 6)	35 (n = 6)	25 (n = 5)	20 (n = 1)
R_i	259.9	1.0	1.050	1.044	0.898	1.023
Ω-cm	± 48.3	±0.017	±0.077	±0.071	±0.079	—
R_m	1,369	1.0	1.429	1.033	0.951	0.979
Ω-cm²	± 189	±0.041	±0.261	±0.093	±0.126	—
C_m	17.4	1.0	0.956	1.055	1.066	0.782
μF/cm²	± 2.2	±0.035	±0.044	±0.063	±0.064	—
ΔV_r	−79.2	0.0	−0.3	−2.4	−2.5	−2.4
mV	± 3.2	±1.0	±1.3	±1.3	±1.2	—

Effect of lowered Na_o on resting membrane properties. Parameters labeled as in text. Units apply only to mean control values except for ΔV_r where mean value is mean V_r, others are change in V_r in mV. All values as mean ±SEM. Average control value of each experiment is averaged to give mean control value. All other values are average of all results in each Na level, after normalizing by control value. Column values in percentage Na, 100% = 161 mM.

TABLE II
EFFECT OF LOWERED $[Na]_o$ ON ACTIVE PROPERTIES

	Mean value ($n = 5$)	Percent Na 100 ($n = 13$)	50 ($n = 6$)	35 ($n = 6$)	25 ($n = 5$)	20 ($n = 1$)
$\bar{V}$	63.3	1.0	0.893	0.849	0.773	0.725
mV	± 2.8	±0.009	±0.021	±0.029	±0.054	—
V_{Pk}	115.9	1.0	0.845	0.754	0.622	0.615
mV	± 4.6	±0.008	±0.015	±0.013	±0.036	—
$\dot{V}_{max}$	519.4	1.0	0.674	0.466	0.253	0.254
V/s	± 67.6	±0.021	±0.039	±0.026	±0.045	—
K	10.8	1.0	0.757	0.591	0.301	0.339
ms^{-1}	± 1.2	±0.018	±0.031	±0.030	±0.046	—
C_f	3.65	1.0	1.108	1.390	2.083	1.718
$\mu F/cm^2$	± 0.71	±0.021	±0.061	±0.132	±0.299	—
θ	2.7	1.0	0.814	0.649	0.414	0.439
m/s	± 0.3	±0.015	±0.023	±0.024	±0.044	—
$\hat{I}$	2904	1.0	0.753	0.697	0.778	0.488
$\mu A/cm^2$	± 882	±0.026	±0.084	±0.098	±0.264	—
P	137	1.0	0.652	0.514	0.352	0.270
$\mu W/cm^2$	± 35	±0.027	±0.069	±0.065	±0.076	—
$\hat{I}/C_f$	761	1.0	0.669	0.492	0.345	0.284
$\mu A/\mu F$	± 110	±0.026	±0.047	±0.032	±0.081	—
P/C_f	37.8	1.0	0.576	0.364	0.169	0.157
$\mu W/\mu F$	± 5.7	±0.028	±0.045	±0.026	±0.039	—

Effect of lowered Na_o on active properties. Parameters labeled as in text. Units apply only to mean control values. All values as mean ±SE. Average control value of each experiment is averaged to give mean control value. All other values are average of all results in each Na level, after normalizing by control value. Column values in percentage Na, 100% = 161 mM.

A relative membrane potential was used, by defining the starting potential as zero.

Curve Fitting

Curve fits were generated for all $\dot{V}(t)$ curves. As described in Methods, the process involved transforming the $\dot{V}$ data and fitting a polynomial in time to the transformed data. The polynomial degree required to fit the transformed data varied from 6 to 9, with less variation of degree among the upstrokes of any one fiber. The fitted $\dot{V}(t)$ curve was obtained from the inverse transform. The noise-smoothing effect was usually minimal for the $\dot{V}$ curve, but often of major value for the $\ddot{V}$ curve. To compare the fits to the data quantitatively, it is useful to look at specific characteristics of the $\dot{V}$ curves. Useful characteristics in comparing two curves are the peak height ($\dot{V}_{max}$), the area under the curve ($\int \dot{V} dt = V_{pk}$), and the potential at which the peak occurs (V), which can be used as an indicator of the curve's skewness. Plotting the fitted values against the data values (Figs. 4, 5) demonstrates that the $\dot{V}_{max}$ and V_{pk} values match very well. The $\bar{V}$ values are not quite as accurate, but most fitted $\bar{V}$ values are <5 mV from the data value. This is a <5% error for a typical upstroke of 100 mV. On the whole, the fitted curves match the data curves closely.

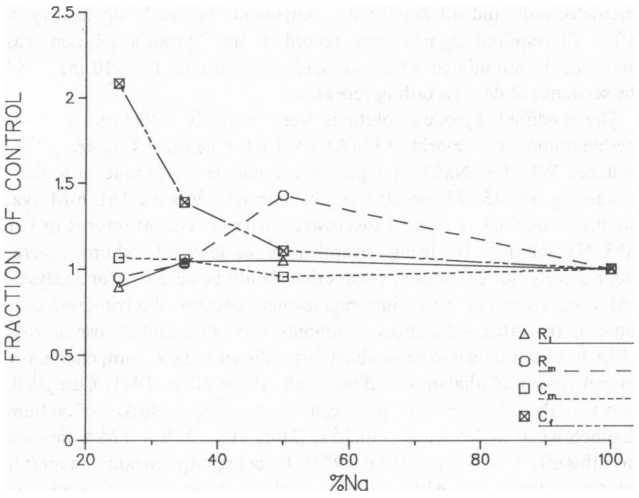

FIGURE 1 Normalized values of cable parameters in solutions of decreased Na_o. Points are average of all normalized values in each Na_o. Lines drawn through points.

From these curve fits, curves of ionic current may be generated. As measures of the curves under the different conditions, values can be obtained for the peak inward (negative) current, $\hat{I}$, and for the upstroke's power ($=\int I_i dV$), designated as P for total area (integrated from $V = 0$ to $V = V_{pk}$). These may be normalized and averaged as for the other upstroke parameters, and are included in Table II and shown in Fig. 6, along with conduction velocity as a reference curve.

A difficulty with these parameters is that unlike values such as θ and $\dot{V}_{max}$, they are expressed as magnitudes per unit area. Because the cable model uses cylindrical surface area, the area used to normalize the total current is

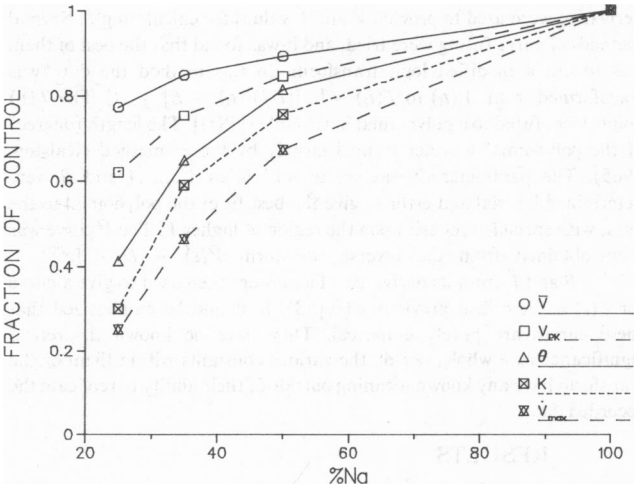

FIGURE 2 Normalized values of upstroke parameters in solutions of decreased Na_o. Points are average of all normalized values in each Na_o. Lines drawn through points.

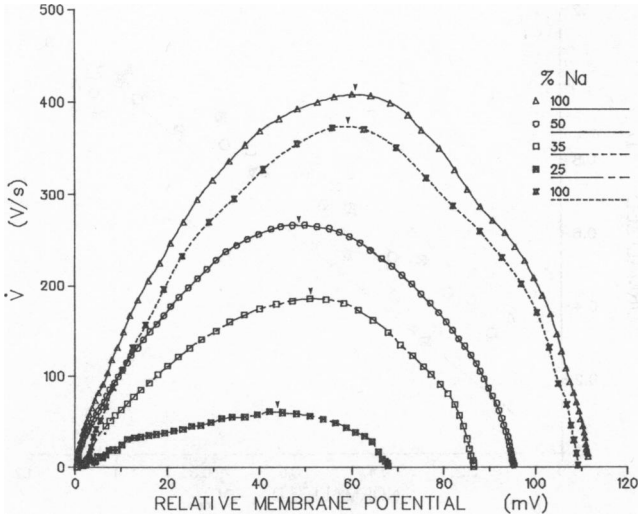

FIGURE 3 Phase plane plots of upstroke velocity curves ($\dot{V}$ as a function of V). Points were obtained by digitizing photographic records of $\dot{V}(t)$ curves in equally spaced time intervals. $V(t)$ curve was digitized at the same position in time. Curves are lines through points. Different curves obtained in different levels of Na_o as marked. Potential at time zero used as 0 mV. Arrows indicate location of points of ($\bar{V}$, $\dot{V}_{max}$).

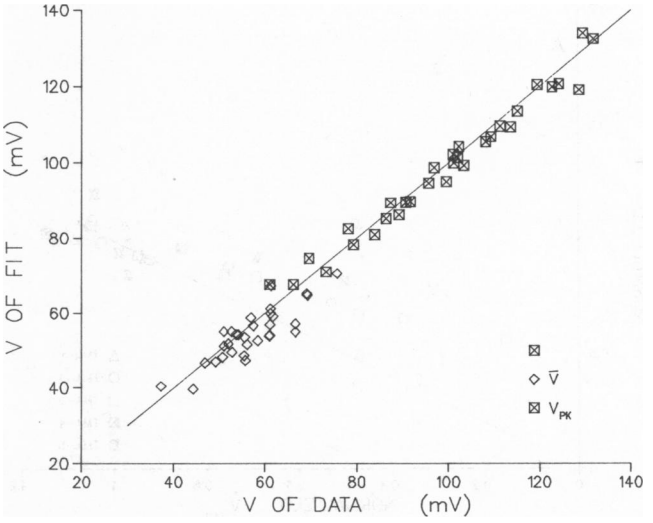

FIGURE 5 Comparison of curve fit values of V_{pk} and $\bar{V}$ to corresponding data values. Straight line is ideal of fitted value equal to data value. Axes cover only range of data obtained.

constant. This is not entirely appropriate. As conduction slows, slower upstrokes will recruit more nonsurface membrane, so that the total membrane area generating ionic current will increase, even though the cylindrical surface area does not. There is no way to measure directly how much area is involved in the upstroke. However, if it is assumed that the membrane capacitance per true unit area is constant in different solutions, then C_f provides a useful indicator of true membrane area involved in the upstroke. The ratio of $\hat{I}/C_f$ will then provide a good indicator of actual changes in peak I_i per true unit area of membrane, and similarly for P/C_f. This ratio also removes the paradoxical result of $\hat{I}$ actually increasing as Na_o declined, due to a large rise in C_f in one experiment. These properly normalized curves (Fig. 6) are seen to fall uniformly and faster than conduction velocity.

$\dot{V}_{max}$ is often used as an experimental indicator of current magnitude. While it is true that in a uniformly polarized membrane the peak net ionic current ($\hat{I}$) is directly proportional to $\dot{V}_{max}$, there is no clear theoretical relationship in the propagated case, because of the increased complexities

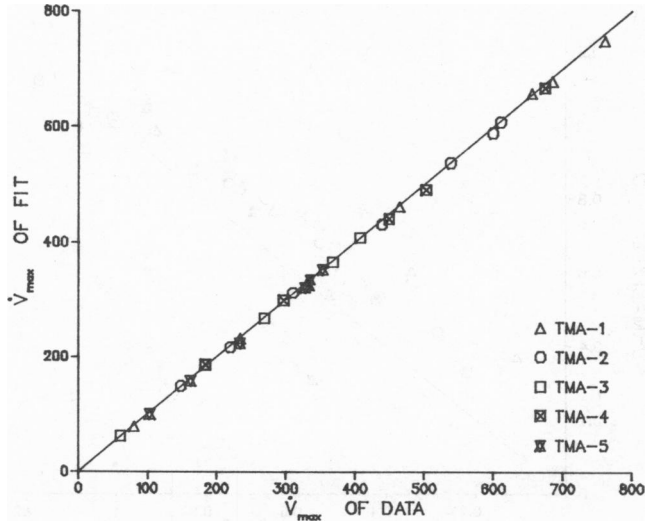

FIGURE 4 Comparison of curve fit values of $\dot{V}_{max}$ to corresponding data value of $\dot{V}_{max}$ for experiments of lowered extracellular sodium. Straight line is ideal of fitted value equal to data value. Different symbols are for individual experiments. Values in units of V/s.

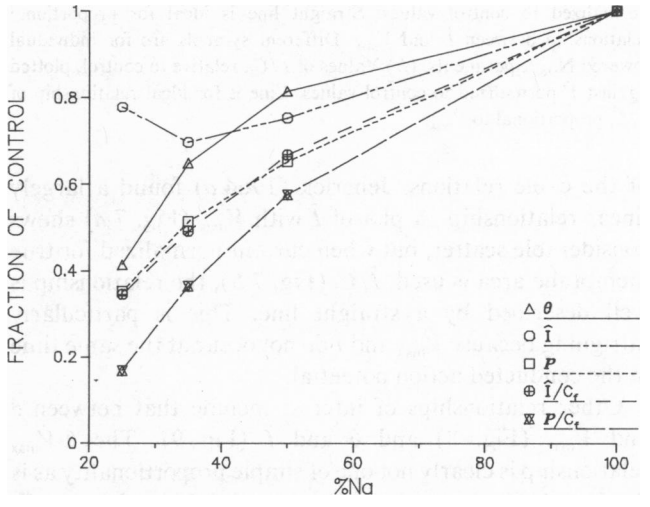

FIGURE 6 Values of peak current and power normalized to control values. Points are averages in each Na_o of peak inward ionic current, $\hat{I}$ and power P. Also shown are curves of normalized $\hat{I}/C_f$ and P/C_f as better indicators of $\hat{I}$ or P for true membrane area (see text). Average conduction velocity curve shown for comparison.

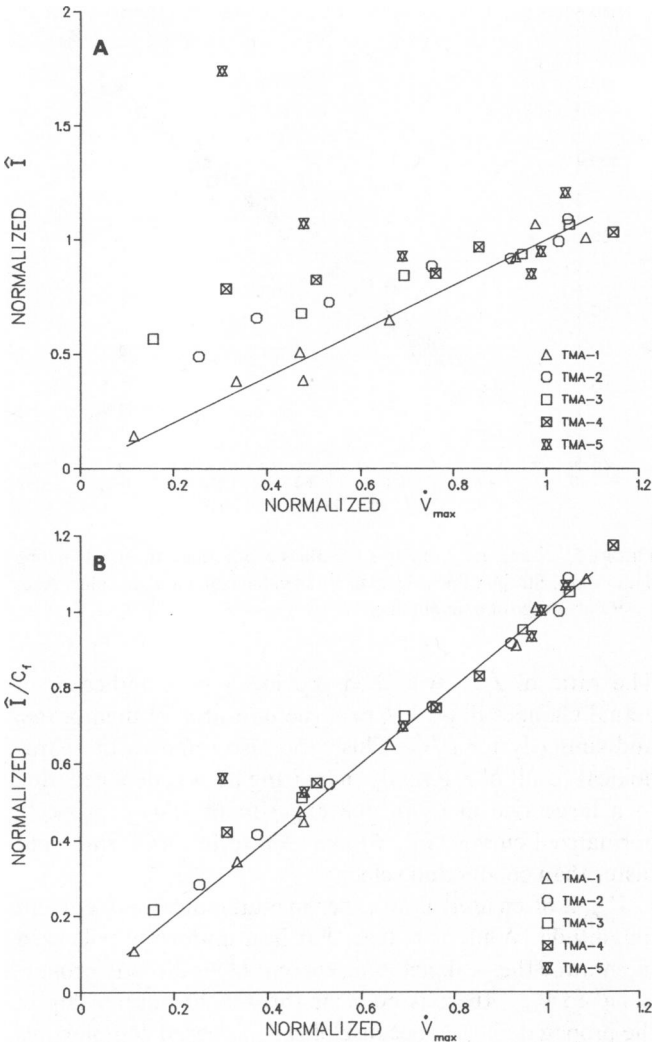

FIGURE 7 (*A*) Peak current, relative to control, plotted against $\dot{V}_{max}$ normalized to control values. Straight line is ideal for proportional relationship between $\hat{I}$ and $\dot{V}_{max}$. Different symbols are for individual lowered Na_o experiments. (*B*) Values of $\hat{I}/C_f$, relative to control, plotted against $\dot{V}$ normalized to control values. Line is for ideal relationship of $\hat{I}/C_f$ proportional to $\dot{V}_{max}$.

of the cable relations. Jenerick (1964 *a*) found a largely linear relationship. A plot of $\hat{I}$ with $\dot{V}_{max}$ (Fig. 7 *a*) shows considerable scatter, but when current normalized for true membrane area is used, $\hat{I}/C_f$ (Fig. 7 *b*), the relationship is well described by a straight line. This is particularly intriguing because $\dot{V}_{max}$ and $\hat{I}$ do not occur at the same time in the conducted action potential.

Other relationships of interest include that between θ and $\dot{V}_{max}$ (Fig. 8) and θ and $\hat{I}$ (Fig 9). The θ-$\dot{V}_{max}$ relationship is clearly not one of simple proportionality as is the $\dot{V}_{max}$-$\hat{I}/C_f$ relationship (the normalized plot does not fit the 1:1 straight line). The greater spread in the data prevent distinguishing between a generally straight-line relationship (which extrapolates to a θ of 20% when $\dot{V}_{max}$ has fallen to 0; that is, when there is no action potential to conduct) or a curved relation of some unknown sort (which

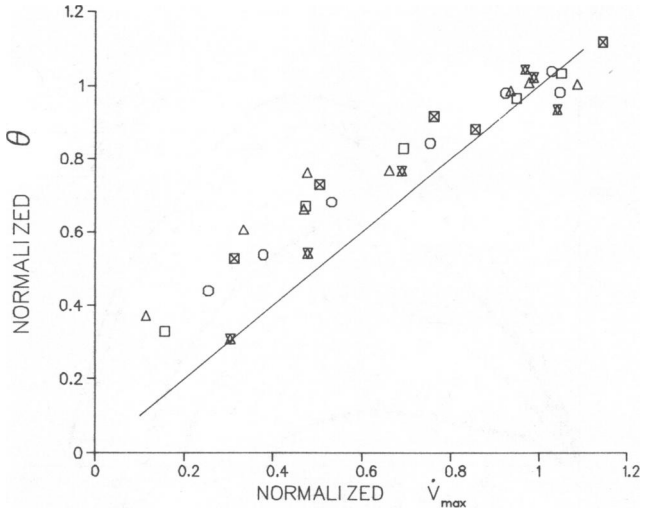

FIGURE 8 Conduction velocity, relative to control, plotted against $\dot{V}_{max}$ normalized to control values. Straight line is ideal for proportional relationship between 0 and $\dot{V}_{max}$. Different symbols for individual experiments.

would allow for θ and $\dot{V}_{max}$ both to coincide at 0). The θ-$\hat{I}/C_f$ relationship, and its indeterminacy, is very similar, as expected from the direct proportionality of the $\dot{V}_{max}$-$\hat{I}/C_f$ relationship.

DISCUSSION

Effect of Lowered Na_o

The effect of lowered external sodium can be approached by considering the basic equations for ion movement across a barrier, as did Goldman (1943) and Hodgkin and Katz (1949). The Nernst-Planck equation relates the net ionic current to two components, diffusion and electric field.

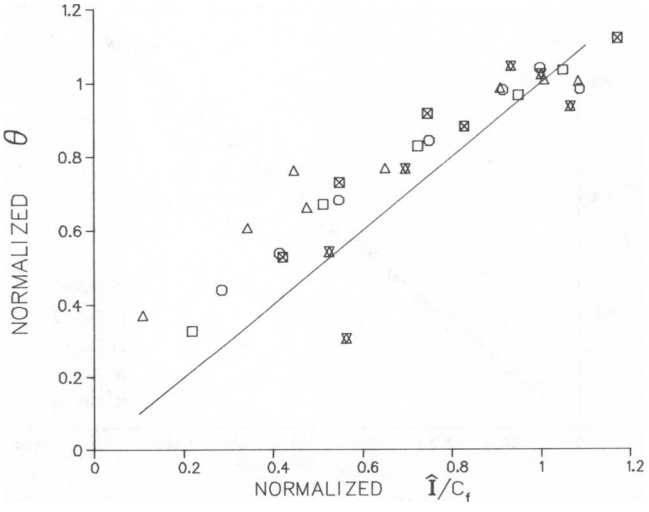

FIGURE 9 Conduction velocity, relative to control, plotted against $\hat{I}/C_f$ normalized to control values. Straight line is ideal for proportional relationship between 0 and $\hat{I}/C_f$. Different symbols for individual experiments.

Assuming that the transmembrane pathway is homogeneous, the electric field is constant throughout the pathway, and the individual ions' movements are independent, then the net current for a positive monovalent ion is

$$I = P\frac{F^2}{RT}\left[\frac{a_o - a_i e^{VF/RT}}{1 - e^{VF/RT}}\right].$$

Inward current is written as negative. F, R, T have their usual meaning, and V is transmembrane potential (inside-outside). a_o and a_i are the activities of the ion species in the outside and inside solutions, and P is a permeability constant. Consider the ratio of the new (I') to previous current (I) when a_o changes. With small a_i and at the same potential below 0 mV so that the exponential term is <1, the ratio may be simplified to $I'/I \sim a_o'/a_o$, meaning that current is proportional to the ion activity. Compared with the purely electrical (ohmic) representation for current, $I = G\cdot(V - V_{rev})$, this analogous to a change in conductance, G, if changes in V_{rev} are ignored. Hence, a decrease in external ion activity causes a decreased current that can be interpreted, roughly, as a similar decrease in conductance. In the Hodgkin-Huxley formulation, this would be a decrease in $\bar{G}_{Na}$, the sodium channel's maximum conductance.

Using ion-sensitive microelectrodes of several different designs, the internal sodium activity has been shown to be ~7 mM in sheep Purkinje fibers (Ellis, 1977; Lee et al., 1980), giving a 15:1 ratio of a_o/a_i. Additionally, Ellis (1977) and Sheu et al. (1980) have shown that when the external sodium is decreased, the internal sodium activity also falls in these small cells with high surface-to-volume ratio, so that V_{rev} remains approximately constant. Considering this, ignoring the effects due to the internal sodium level is a reasonable appproximation, and should not cause a large error in equating a decreased external sodium to a proportional decrease in sodium conductance.

An additional possible effect of lowered sodium should be considered. Cardiac tissue contains a sodium-calcium exchange system that couples the ratio of the sodium activities to that of the calcium activities. The Na/Ca exchange acts to utilize the sodium gradient to maintain a low intracellular calcium level. If external sodium is lowered, the initial expectation might be decreased activity of the exchange mechanism, allowing a rise in internal calcium. This might influence conduction because of the effect of calcium to decrease coupling between cardiac cells (Délèze, 1970; DeMello, 1975). In these experiments R_i remained constant. This result is at least in part due to the decline in internal Na, so that the ratio of sodium activities was changed only slightly. Even though the absolute magnitude of the activities has declined, it is the ratio that acts to influence the steady-state exchange activity. With the ratio nearly constant, the rise in internal calcium activity will be limited to a much smaller amount. The experiments of Sheu and Fozzard (1982) using a Ca-sensitive microelectrode to monitor internal calcium activity suggest that in the low Na_o solutions used in these experiments, it rose to 300–400 nM ($[Ca]_i$ of ~1 μM). Consequently, this must be below the level necessary to affect R_i (Weingart, 1977; Dahl and Isenberg, 1980).

Effect on Upstroke Parameters

Experiments with reduced external sodium have been performed on other tissues. Hodgkin and Katz (1949) worked with squid giant axon and obtained results qualitatively similar to those obtained here. Both action potential height and $\dot{V}_{max}$ showed a nonlinear decline, with increasing sensitivity in the lower sodium solutions. V_{pk} was seen by them to be much less sensitive than $\dot{V}_{max}$ as was obtained here. They did not measure θ systematically.

Hardy (1973) has looked at the effect of lowered sodium levels on frog myelinated nerve. He looked only at conduction velocity and found that it varied approximately as $\sqrt{Na_o}$. This was contrary to the results seen here, where θ declined less than proportional to $\sqrt{Na_o}$ at first, and then accelerated its decline in the lower Na solutions. Extrapolation of the curve shows failure of conduction (θ falls to 0) at a sodium concentration above 0, unlike extrapolation of Hardy's curve. The relation of Hardy's studies to the results obtained here is uncertain, because of the different types of conduction studied.

It is useful to review what relationships are already widely recognized. In a segment of isolated, uniformly polarized membrane, $\dot{V}$ is proportional to I_i/C_f at all times, hence $\dot{V}_{max}$ is proportional to $\hat{I}/C_f$. For a propagating action potential, the cable relations are much more complex. Although it is widely accepted that if $\hat{I}/C_f$ increases, $\dot{V}_{max}$ will increase, it has not been at all clear what quantitative relationship occurs between them, especially as they occur at different times. The only quantitative relationship available is between K and θ. By utilizing the cable relations with the assumption of negligible outward current in the foot, it can be shown (Tasaki and Hagiwara, 1957) that $K = 2R_iC_f\theta^2/a$. Beyond these two relations, of which only one is quantitative, there are no widely recognized ones.

Jenerick (1964 *a*) experimentally found $\hat{I}$ to be directly proportional to $\dot{V}_{max}$; our study agrees with this result. The relationship between θ and $\dot{V}_{max}$ was a different situation. The general expectation was that they will both be affected by interventions in a similar direction, and this did occur. However, they did not change in a proportional manner, and a noticeable amount of the variation in one was not related to variation in the other (spread of the data along the overall trend), indicating that there are factors that can influence one parameter and not the other. What the form of the actual overall trend is and what other factors may be involved in their relationship cannot be determined from these data.

This difficulty points out the problem of relying only on experimental results for insight into the conduction pro-

cess. This problem occurs even with the $\dot{V}_{max}$-$\hat{I}/C_f$ relationship. Empirically, a straight line reproduces the data well, and is generally sufficient for any practical application of the data. However, the data cannot distinguish between a true linear relationship and a curve that merely falls near the straight line for the range of variation seen. Also, insight is not provided into whether or not there are other factors that can also influence this relationship, which happened to have remained constant under the conditions utilized in this study. Ideally, the variables should be related to the description of membrane channels and their specific properties as described by voltage clamp experiments (Hodgkin and Huxley, 1952). The use of models is designed to approach some of these questions. There are many different types of models, and it will be seen in the second paper of this set that models are able to provide insight into the interpretation of the data obtained in these experiments.

The work for this paper was supported by U.S. Public Health Service grants HL20592 and HD-07009.

Received for publication 22 June 1982 and in revised form 5 May 1983.

REFERENCES

Cahalan, M., and T. Begenisich. 1976. Sodium channel selectivity depending on internal permeant ion concentration. *J. Gen. Physiol.* 68:111–125.

Campbell, D. T. 1976. Ionic selectivity of the sodium channel of frog skeletal muscle. *J. Gen. Physiol.* 67:295–307.

Cole, K. S., and H. J. Curtis. 1938. Electrical impedance of nitella during activity. *J. Gen. Physiol.* 22:37–64.

Dahl, G., and G. Isenberg. 1980. Decoupling of heart muscle cells: correlation with increased calcium activity and with changes of nexus ultrastructure. *J. Membr. Biol.* 53:63–75.

Délèze, J. 1970. The recovery of resting potential and input resistance in sheep heart injured by knife or laser. *J. Physiol. (Lond.).* 208:547–562.

DeMello, W. C. 1975. Effect of intracellular injection of calcium and strontium on cell communication in heart. *J. Physiol. (Lond.).* 250:231–245.

Ellis, D. 1977. The effects of external cations and ouabain on the intracellular sodium activity of sheep heart Purkinje fibers. *J. Physiol. (Lond.).* 273:211–240.

Fozzard, H. A. 1966. Membrane capacity of the cardiac Purkinje fiber. *J. Physiol. (Lond.).* 182:255–267.

Fozzard, H. A. 1979. Conduction of the action potential. *In* Handbook of Physiology: The Cardiovascular System I. The Heart. R. M. Berne, editor. American Physiological Society. Bethesda, MD. 335–356.

Fozzard, H. A., and M. Schoenberg. 1972. Strength-duration curves in cardiac Purkinje fibers: Effects of liminal length and charge distribution. *J. Physiol. (Lond.).* 226:593–618.

Freygang, W. H., and W. Trautwein. 1970. The structural implications of the linear electrical properties of cardiac Purkinje strands. *J. Gen. Physiol.* 55:524–547.

Goldman, D. E. 1943. Potential, impedance, and rectification in membranes. *J. Gen. Physiol.* 27:37–60.

Hardy, W. L. 1973. Propagation speed in myelinated nerve. I. Experimental dependence on external Na^+ and on temperature. *Biophys. J.* 13:1054–1070.

Hille, B. 1971. The permeability of the sodium channel to organic cations in myelinated nerve. *J. Gen. Physiol.* 58:599–619.

Hille, B. 1975. Ionic selectivity, saturation, and block in sodium channels. A four-barrier model. *J. Gen. Physiol.* 66:535–560.

Hodgkin, A. L., and A. F. Huxley. 1952. A quantitative description of membrane current and its application to conduction and excitation in nerve. *J. Physiol. (Lond.).* 117:500—544.

Hodgkin, A. L., and B. Katz. 1949. The effect of sodium ions on the electrical activity of the giant axon of the squid. *J. Physiol. (Lond.).* 108:57–77.

Hodgkin, A. L., and W. A. H. Rushton. 1946. The electrical constants of a crustacean nerve fiber. *Proc. R. Soc. Lond. B. Biol. Sci.* 133:444–479.

Horn, R., J. Patlak, and C. F. Stevens. 1981. The effect of tetramethylammonium on single sodium channel currents. *Biophys. J.* 36:321–327.

Jenerick, H. 1963. Phase plane trajectories of the muscle spike potential. *Biophys. J.* 3:363–377.

Jenerick, H. 1964 *a*. An analysis of the striated muscle fiber action current. *Biophys. J.* 4:77–91.

Jenerick, H. 1964 *b*. Letter to the Editor. *Biophys. J.* 4:251–255.

Lee, C. O., D. H. Kang, J. H. Sokol, and K. S. Lee. 1980. Relation between intracellular Na ion activity and tension of sheep cardiac Purkinje fibers exposed to dihydro-ouabain. *Biophys. J.* 29:315–330.

Levin, D. N., and H. A. Fozzard. 1981. A cleft model for cardiac Purkinje strands. *Biophys. J.* 33:383–408.

Ralston, A. 1965. A First Course in Numerical Analysis. McGraw-Hill, Inc., New York.

Rosenblueth, A., N. Wiener, W. Pitts, and J. G. Ramos. 1948. An account of the spike potential of axons. *J. Cell. Comp. Physiol.* 32:275–317.

Sheu, S.-S., M. Korth, D. A. Lathrop, and H. A. Fozzard. 1980. Intra- and extracellular K^+ and Na^+ activities and resting membrane potential in sheep cardiac Purkinje strands. *Circ. Res.* 47:692–700.

Sheu, S.-S., and H. A. Fozzard. 1982. Transmembrane Na^+ and Ca^{2+} electrochemical gradients in cardiac muscle and their relationship to force development. *J. Gen. Physiol.* 80:325–351.

Tasaki, I., and S. Hagiwara. 1957. Capacity of muscle fiber membrane. *Am. J. Physiol.* 188:423–429.

Weidmann, S. 1952. The electrical constants of Purkinje fibers. *J. Physiol. (Lond.).* 118:348–360.

Weingart, R. 1977. The actions of ouabain on intracellular coupling and conduction velocity in mammalian ventricular muscle. *J. Physiol. (Lond.).* 264:341–356.